Mantle strength of the San Andreas fault system and the role of mantle-crust feedbacks

Vasileios Chatzaras[1,2], Basil Tikoff[1], Julie Newman[3], Anthony C. Withers[4], and Martyn R. Drury[2]
[1]Department of Geoscience, University of Wisconsin–Madison, Madison, Wisconsin 53706, USA
[2]Department of Earth Sciences, Utrecht University, PO Box 80.021, 3508 TA Utrecht, Netherlands
[3]Department of Geology and Geophysics, Texas A&M University, College Station, Texas 77843, USA
[4]Department of Earth Sciences and the Centre for Planetary Science and Exploration, University of Western Ontario, 1151 Richmond Street, London, Ontario N6A 5B7, Canada

ABSTRACT

In lithospheric-scale strike-slip fault zones, upper crustal strength is well constrained from borehole observations and fault rock deformation experiments, but mantle strength is less well known. Using peridotite xenoliths, we show that the upper mantle below the San Andreas fault system (California, USA) is dry and its maximum resolved shear stress (5–9 MPa) is similar to the shear strength of the upper, seismogenic portion of the fault. These results do not fit with any existing lithospheric strength profile. We propose the "lithospheric feedback" model in which the upper crust and lithospheric mantle act together as an integrated system. Mantle flow controls displacement and loads the upper crust. In contrast, the upper crust controls the stress magnitude in the integrated system. Crustal rupture transiently increases strain rate in the upper mantle below the strike-slip fault, leading to viscous strain localization. The lithospheric feedback model suggests that lithospheric strength is a dynamic property—varying in space and time—in actively deforming regions.

INTRODUCTION

The strength of the San Andreas fault (SAF) system (California, United States) has been a topic of considerable interest, and controversy, for over three decades. The strength of the crustal section of the SAF was proposed to be extremely weak (Zoback et al., 1987), based on the lack of a heat flow anomaly and the inferred orientation of maximum compressive stress at high angle to the strike of the fault. Stress drops of <10 MPa, associated with earthquakes in the seismogenic upper crust, are consistent with low shear strength (Scholz, 2000). Frictional properties of San Andreas Fault Observatory at Depth core samples suggest that the shear strength of the SAF is 10–17 MPa (Lockner et al., 2011; Carpenter et al., 2012) and should remain constant in the upper 5–8 km of the crust (Carpenter et al., 2012).

The rheologies of the lower crust and upper mantle within the SAF system are more difficult to quantify. Experimental rock deformation studies have generally constrained the strength of the lithosphere; rock rheology depends on composition as well as grain size, temperature, pressure, and water content (Kohlstedt et al., 1995). Through characterization of the relative strength of the different lithospheric layers, a series of conceptual lithospheric strength profiles were developed (jelly sandwich, crème brûlée, banana split; Bürgmann and Dresen, 2008). For the SAF, different workers have suggested that either the upper crust (Pollitz et al., 2001) or the upper mantle (Molnar, 1992) control lithospheric strength.

Most conceptualizations of lithospheric strength require that the different lithospheric layers are independent of each other and that the rheology of each layer is constant through time. This former assumption overlooks the observation that crustal deformation in the SAF continues into the lithospheric mantle (Henstock et al., 1997; Titus et al., 2007) and possibly to the asthenosphere (Ford et al., 2014). The latter assumption overlooks that deformation in viscous shear zones below major strike-slip faults is unlikely to occur at constant strain rates, particularly given the evidence for rapid-slip events in the lower crust (Regan et al., 2014).

In this study, we utilize deformed mantle xenoliths that sample the Calaveras fault of the SAF system in order to determine the strength of the mantle below an active plate-bounding strike-slip fault. Evidence from the mantle xenoliths allows us to study the SAF as an integrated lithospheric-scale system and assess the role of mantle and crustal deformation during the seismic cycle. The proposed lithospheric feedback model provides a possible mechanism to explain apparently contradictory data about the SAF system in a coherent, systematic way.

ANALYSIS OF SAF MANTLE XENOLITHS

A suite of ultramafic xenoliths found in the Coyote Lake basalt was described by Titus et al. (2007). The Coyote Lake basalt is located near the intersection of the Hayward and Calaveras faults in central California (Fig. 1A), and is interpreted to result from intrusion into a small pull-apart system at ca. 3 Ma (Nakata et al., 1993; Jové and Coleman, 1998). The analyzed mantle xenoliths are spinel harzburgites and lherzolites (Fig. DR1 in the GSA Data Repository[1]), which equilibrated at temperatures of 970–1100 °C and estimated depths of 37.8–42.5 km (Titus et al., 2007). Crystallographic preferred orientations (CPOs) of olivine exhibit strong

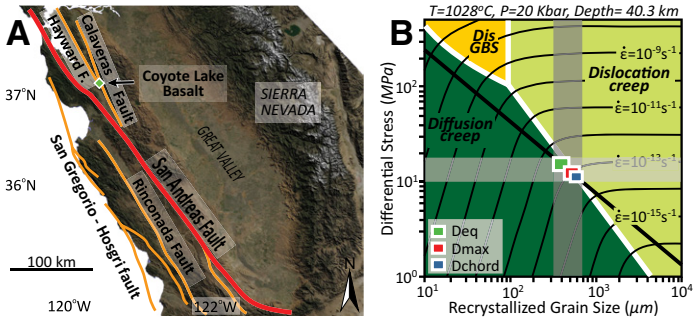

Figure 1. Location of San Andreas fault (SAF) mantle xenoliths and deformation mechanism map for dry olivine. A: Map of central California (USA) showing location of Coyote Lake volcanic field (terrain map from www.gelib.com/global-terrain-map.htm). Red indicates SAF; orange indicates subsidiary active fault strands. B: Deformation mechanism map for dry olivine at mean deformation conditions experienced by the xenolith suite. Grain-size data are plotted on line corresponding to linear least squares fit to data of Karato et al. (1980) and Van der Wal et al. (1993), based on Warren and Hirth (2006). Colored boxes correspond to the range of calculated differential stress based on measured recrystallized grain size using: Dchord—linear intercept method; Dmax—maximum diameter method; Deq—equivalent area diameter method. *T*—temperature; *P*—pressure; $\dot{\varepsilon}$—strain rate; DisGBS—dislocation-accommodated grain boundary sliding.

[1]GSA Data Repository item 2015299, Figure DR1 (San Andreas fault mantle xenoliths); Figure DR2 (FTIR spectra from olivine and orthopyroxene); Figure DR3 (feedback loop of the lithospheric feedback model for western California); and Table DR1 (paleopiezometry results), is available online at www.geosociety.org/pubs/ft2015.htm, or on request from editing@geosociety.org or Documents Secretary, GSA, P.O. Box 9140, Boulder, CO 80301, USA.

[100] point maxima and indicate that deformation was dominantly accommodated by dislocation creep (Titus et al., 2007). Significantly, the very strong olivine CPO patterns suggest that mantle shearing occurred below the Calaveras fault at depths of ~40 km.

Our new water-content and grain-size data put quantitative constraints on the hydration and stress state of the deforming upper mantle below the SAF during shearing. Fourier transform infrared spectroscopic measurements determined the H content of both olivine and orthopyroxene in the Coyote Lake basalt xenoliths. Average H contents are <2 ppm H_2O (<20 H/10^6 Si) in olivine and ~32 ppm H_2O (400 H/10^6 Si) in orthopyroxene (Fig. DR2). Olivine in mantle xenoliths is susceptible to diffusive loss of H during emplacement, while orthopyroxene has been shown to preserve its pre-emplacement H content with greater fidelity (Warren and Hauri, 2014). We use the equilibrium partition coefficient for H between orthopyroxene and olivine, $D^{opx/ol}$, to determine the pre-emplacement H content of the olivine. Experiments show that $D^{opx/ol}$ is strongly dependent upon the Al_2O_3 content of the orthopyroxene (Hirschmann et al., 2009). The Al_2O_3 content of the orthopyroxene, determined by electron microprobe analysis, is 4.4 wt%, from which we estimate $D^{opx/ol}$ to be <10 (Ardia et al., 2012). Consequently, prior to emplacement, the olivine had a maximum H content of ~3 ppm H_2O (one-tenth of the orthopyroxene H content). Hence, the upper mantle below the Calaveras fault is dry.

Olivine recrystallized grain size was measured in seven samples using the linear intercept, maximum diameter, and equal-area diameter methods. A correction factor of 1.75 was applied for the linear intercept and 1.2 for the maximum and equal-area diameter methods to account for two-dimensional sectioning of spherical grains (Drury, 2005). The geometric means of the recrystallized grain size distributions for the seven samples obtained by the three methods range from 320 to 712 µm (Table DR1). Using the empirical piezometric relationships proposed for olivine deformed under dry conditions (Karato et al., 1980; Van der Wal et al., 1993) we estimate differential stresses of 9.8–17.8 MPa from the olivine recrystallized grain size (Table DR1). Assuming simple shear deformation, the shear stress is one-half of the differential stress, and thus 4.9–8.9 MPa. To calculate strain rate, we use the experimentally derived flow law, $\dot{\varepsilon} = A\sigma^n d^{-m} f_{H_2O}^r e^{-\frac{(Q+PV)}{RT}}$, where $\dot{\varepsilon}$ is strain rate, A is a material constant, σ is differential stress, n is the stress exponent, d is the recrystallized grain size, m is the grain-size exponent, $f_{H_2O}^r$ is water fugacity, Q is activation energy, P is pressure, V is activation volume, R is the molar gas constant, and T is temperature. Using the values of the flow law parameters for dry olivine (Hirth and Kohlstedt, 2003), we constrain upper mantle strain rates below the fault zone to 8.1 × 10^{-15} to 5.0 × 10^{-13} s^{-1} (Fig. 1B; Table DR1). Grain size data plot on the boundary between the dislocation creep and diffusion creep fields using the olivine paleopiezometer (Fig. 1B). Assuming simple shear deformation, we estimate the viscosity of the sheared mantle in the range of 7.0 × 10^{18} to 3.1 × 10^{20} Pa·s.

The critical result from the SAF xenoliths is that the shear stress (~5–9 MPa) of the lithospheric mantle is comparable to the crustal strength (~10 MPa) of seismogenic strike-slip faults in the SAF system (Fig. 2B). Such strength similarity suggests that deformation in these two lithospheric layers might be mechanically linked (Fig. 2A). This result is supported by inferences of mantle-crust coupling worldwide along major strike-slip shear zones (Vauchez et al., 2012).

Comparison with Other Studies

Our results are generally consistent with a recent study of mantle xenoliths from the Cima volcanic field, southern California (Behr and Hirth, 2014). This study analyzed mantle xenoliths from shallower depths, inferred to have been extracted from directly below the Moho (equilibration temperatures of 850–950 °C). The calculated differential stresses (13–17 MPa) and viscosity (3 × 10^{19} Pa·s) from this study are directly comparable to those of the SAF xenoliths (Fig. 2B). Another comparison can be made to the ~5-km-wide Bogota Peninsula shear zone, New Caledonia, which is interpreted as the mantle section of a strike-slip fault. Deformation in this shear zone occurred at ~900 °C (Prinzhofer and Nicolas, 1980), and the differential stresses (15–19 MPa) are again similar to those of the SAF (Chatzaras et al., 2014). These two studies support the contention that the uppermost mantle below strike-slip faults records relatively low differential stress.

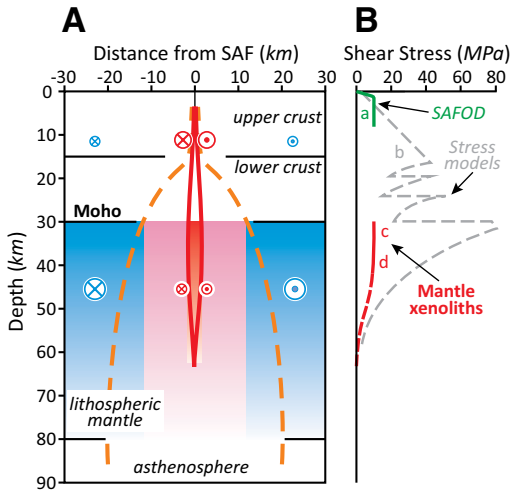

Figure 2. Mantle-crust feedbacks and lithospheric strength in San Andreas fault (SAF). A: Vertical profile across SAF showing lateral extent of areas in lithospheric mantle controlled by each of two opposing mechanisms: mantle flow (blue) and crustal rupture (red). Pink area alternates between being more affected by mantle displacement (interseismic period) and crustal displacement (rupture and post-seismic stages). Vectors (in [x] and out [dot] of page) are scaled in size to represent relative movement between different lithospheric levels during interseismic flow (blue) or immediately following crustal fault slip (red) (see text for details). B: Shear stress versus depth profile. Data are from: a—Carpenter et al. (2012); b—Humphreys and Coblentz (2007); c—Behr and Hirth (2014); d—this study. SAFOD—San Andreas Fault Observatory at Depth.

LITHOSPHERIC FEEDBACK MODEL

Existing rheological models for western California do not adequately explain the new SAF xenolith results. The jelly sandwich and crème brûlée models do not predict similar stress in the crust and mantle (Bürgmann and Dresen, 2008). The banana split model predicts an upper mantle of low strength below the fault zone, but requires the operation of a strain-weakening mechanism, such as addition of water in the system or deformation by diffusion creep. However, xenolith data indicate dry conditions and exhibit strong olivine CPOs, supporting deformation dominantly by dislocation creep (Titus et al., 2007).

We propose the "lithospheric feedback" model as an alternative rheological model for lithospheric-scale strike-slip fault zones. The essence of the lithospheric feedback model is that viscous mantle deformation and frictional crustal deformation in fault zones are mechanically coupled but have opposite rheological tendencies. The viscous deformation within the mantle effectively distributes deformation over large areas, while frictional deformation (e.g., seismic events) within the crust localizes deformation in very narrow zones. The effect of these differences is twofold: (1) mantle flow causes widespread crustal deformation and displacement loading; and (2) crustal deformation by fault rupture causes displacement rate loading and strain localization in the upper mantle (and lower crust) below strike-slip faults. Thus, the issue is not the relative strength of the

mantle or crust; rather, the important question is how the lithospheric layers interact with each other during the seismic cycle.

The Seismic Cycle

Figure 3 describes the spatiotemporal evolution of displacement and stress within different lithospheric levels during a seismic cycle, as predicted by the lithospheric feedback model. In the pre-rupture stage, mantle flow provides the displacement loading that ultimately causes the crustal rupture. Viscous flow in the mantle occurs throughout western California across a 130-km-wide area underneath both the faults and the borderlands (rock volumes between major faults), as denoted by shear wave splitting studies (e.g., Ozalaybey and Savage, 1995). Mantle flow effectively loads the crust by traction and slowly builds stress within both the faults and the borderlands (Fig. 3A). When stress in the fault zone exceeds the ~10 MPa shear strength of the SAF, the upper-crustal portion of the fault ruptures in narrow zones.

The effect of rapid and localized crustal rupture on the underlying mantle is a transient increase in its strain rate, and therefore stress (Fig. 3B). The horizontal displacement profile is characterized by a steep gradient below the crustal portion of the fault, although the mantle portion retains continuity (Fig. 3B). Localized mantle flow in the shear zone occurs synchronously with the distributed mantle flow throughout western California at lower strain rates.

During the post-seismic period, the lithospheric mantle responds to the displacement rate loading from the crust by viscously dissipating the increased stress and redistributing displacement into a wider zone. Transient mantle flow is responsible for the post-seismic crustal creep, distributed over hundreds of kilometers, as recorded after the Mohave earthquakes in California (Freed et al., 2012). Viscous materials generally respond to localized deformation by effectively widening the sheared zone, which lowers the maximum shear zone strain rate and elevates the surrounding strain rate (Vauchez et al., 2012) (Figs. 2A and 3C).

If the stress conditions in the mantle change during the earthquake cycle, it is reasonable to ask whether the mantle xenoliths record the maximum stress (occurs during the rupture), the minimum stress, or a long-term average. We suspect that the xenoliths record the maximum stress for three reasons. First, most deformation will occur close to the maximum stress conditions, when the strain rate is fastest in a viscous material. Second, the maximum stress results in a small olivine grain size. Any increase in the grain size—which is necessary to record lower stresses—is through annealing, which is likely to be relatively limited in dry olivine on the time scale of the ~100 yr seismic cycle. Third, pseudotachylytes and fine-grained ultramylonites— rocks typically associated with high strain rates—are not observed in the xenolith suite. It is possible that such rocks exist below the SAF but were not sampled by the Coyote Lake basalt. Pseudotachylytes and fine-grained ultramylonites are also absent from the mantle section of other lithospheric-scale strike-slip faults (e.g., Bogota Peninsula shear zone, New Caledonia; Titus et al., 2011).

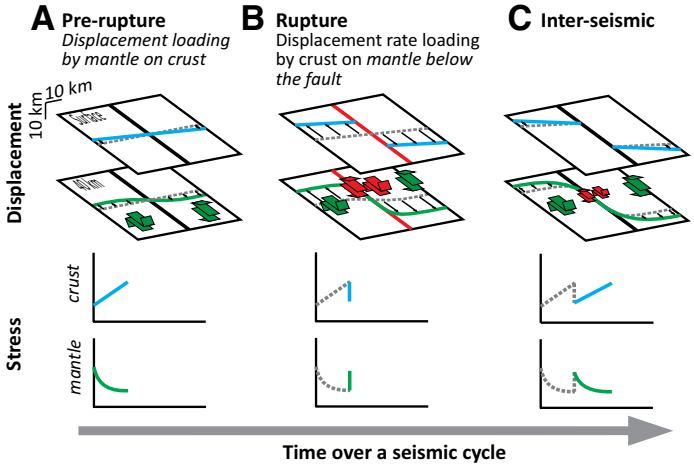

Figure 3. Evolution of displacement (upper panel) and stress (lower panel) during a seismic cycle, as predicted by the lithospheric feedback model. Displacement evolution is shown in blocks (horizontal slices through upper crust and lithospheric mantle at extraction depth of San Andreas fault mantle xenoliths). Stress variation is shown in stress versus time plots. Gray dotted lines correspond to deformation (upper panel) and stress (lower panel) state at beginning of each step. The lithospheric mantle always has greater displacement than the overlying crust, except within the shear zone during a rupture event when crustal displacement rate loading occurs.

How does the upper crustal segment of the fault control the stresses in the upper mantle? Freed et al. (2012) modeled stress loading of the upper mantle portion of the fault resulting from co-seismic slip in the upper crust. The result indicated very low magnitudes (<< 1 MPa) of increasing stress, suggesting that stress loading is not a viable mechanism. An alternative mechanism is displacement rate loading of the upper mantle. In a coupled lithospheric system, such as the SAF, fault slip in the upper crust necessarily results in viscous displacement along a connected ductile shear zone (Teyssier and Tikoff, 1998) (Figs. 2A and 3B). This increase in the strain rate within the mantle shear zone will necessarily increase the stress. This inference of rheological behavior is supported by field studies that document increased stress magnitudes in portions of mantle shear zones that experienced higher strain and/or strain rates (Michibayashi et al., 2006; Chatzaras et al., 2014).

Role of the Lower Crust

The lithospheric feedback model requires that the lower crust kinematically couples the upper crust and lithospheric mantle. Further, displacement rate loading suggests that the lower crust fluctuates in its behavior between (1) rupture and rapid movement during seismic slip and post-seismic deformation, and (2) slower movement during the interseismic period. This interpretation is consistent with studies of lower crustal shear zones, which exhibit pseudotachylyte (indicating seismic rupture) and ultramylonites within larger mylonitic zones (Regan et al., 2014). Geophysical studies along the SAF also support this notion of different types of deformation behavior in the lower crust. The deep (20–30 km) focal depth distribution of low-frequency earthquakes below the SAF suggests propagation of seismogenic rupturing down to the lower crust (Shelly, 2015). On the other hand, post-seismic relaxation studies (Pollitz et al., 2001) and experimental flow laws (Rybacki and Dresen, 2004) suggest viscous creep of the lower crust. These data might not be in conflict; the lower crustal portion of the SAF might be characterized by an alternation of rapid and slow movement. Moreover, the behavior of the lower crust is clearly time dependent. Based on post-seismic deformation studies in California, Pollitz et al. (2001) concluded that the lower crust adjusts its rheology and acts as a stress guide, as a result of effectively coupling deformation in the upper crust and upper mantle.

Applicability of the Lithospheric Feedback Model

We note that our model is specifically for vertical strike-slip systems, which exhibit continuity in the lithosphere. The lithospheric feedback model may not apply to deformation in extension and/or contraction settings because of the horizontally layered nature of the lithosphere. The converse is also true; estimates of lithospheric strength in extension and/or contraction settings (e.g., Behr and Platt, 2014) may not be applicable to strike-slip systems.

CONCLUSIONS

Mantle xenoliths from below the SAF system record very low water content (~3 ppm) and differential stress of 10–18 MPa (maximum resolved shear stress of 5–9 MPa). These results are not consistent with any existing

lithospheric strength profile. In order to explain these observations, we propose the lithospheric feedback model, which suggests that the lithospheric strength of the SAF system is controlled by the rheological interaction of the upper crust and upper mantle, which together act as an integrated system: mantle deformation controls the displacement, and upper crustal deformation controls the stress magnitude. The lithospheric feedback model suggests that the time-dependent interaction of the rheologically distinct lithospheric layers—rather than their relative strengths—is the critical parameter that governs the behavior of the SAF system.

ACKNOWLEDGMENTS

We thank Clark Johnson for supplying samples of the mantle xenoliths from the Coyote Lake basalt. We thank L. Gordon Medaris and Sarah J. Titus for helpful comments. Constructive comments from Whitney Behr and two anonymous reviewers are highly appreciated. This work was supported by a Marie Curie International Outgoing Fellowship to Chatzaras (PIOF-GA-2012-329183).

REFERENCES CITED

Ardia, P., Hirschmann, M.M., Withers, A.C., and Tenner, T.J., 2012, H_2O storage capacity of olivine at 5–8 GPa and consequences for dehydration partial melting of the upper mantle: Earth and Planetary Science Letters, v. 345–348, p. 104–116, doi:10.1016/j.epsl.2012.05.038.

Behr, W.M., and Hirth, G., 2014, Rheological properties of the mantle lid beneath the Mojave region in southern California: Earth and Planetary Science Letters, v. 393, p. 60–72, doi:10.1016/j.epsl.2014.02.039.

Behr, W.M., and Platt, J.P., 2014, Brittle faults are weak, yet the ductile middle crust is strong: Implications for lithospheric mechanics: Geophysical Research Letters, v. 41, p. 8067–8075, doi:10.1002/2014GL061349.

Bürgmann, R., and Dresen, G., 2008, Rheology of the lower crust and upper mantle: Evidence from rock mechanics, geodesy, and field observations: Annual Review of Earth and Planetary Sciences, v. 36, p. 531–567, doi:10.1146/annurev.earth.36.031207.124326.

Carpenter, B.M., Saffer, D.M., and Marone, C., 2012, Frictional properties and sliding stability of the San Andreas fault from deep drill core: Geology, v. 40, p. 759–762, doi:10.1130/G33007.1.

Chatzaras, V., Titus, S., Tikoff, B., and Drury, M.R., 2014, Microstructural and rheological constraints on the mantle strength of strike-slip fault systems: Evidence from the Bogota Peninsula shear zone, New Caledonia, *in* Proceedings, 2014 American Geophysical Union Fall Meeting, San Francisco, California, 15–19 December, Abstract T31A–4576.

Drury, M.R., 2005, Dynamic recrystallization and strain softening of olivine aggregates in the laboratory and the lithosphere, *in* Gapais, D., et al., eds., Deformation Mechanisms, Rheology and Tectonics: From Minerals to the Lithosphere: Geological Society of London Special Publication 243, p. 143–158, doi:10.1144/GSL.SP.2005.243.01.11.

Ford, H.A., Fischer, K.M., and Lekic, V., 2014, Localized shear in the deep lithosphere beneath the San Andreas fault system: Geology, v. 42, p. 295–298, doi:10.1130/G35128.1.

Freed, A.M., Hirth, G., and Behn, M.D., 2012, Using short-term postseismic displacements to infer the ambient deformation conditions of the upper mantle: Journal of Geophysical Research, v. 117, B01409, doi:10.1029/2011JB008562.

Henstock, T.J., Levander, A., and Hole, J.A., 1997, Deformation in the lower crust of the San Andreas fault system in northern California: Science, v. 278, p. 650–653, doi:10.1126/science.278.5338.650.

Hirschmann, M.M., Tenner, T.J., Aubaud, C., and Withers, A.C., 2009, Dehydration melting of nominally anhydrous mantle: The primacy of partitioning: Physics of the Earth and Planetary Interiors, v. 176, p. 54–68, doi:10.1016/j.pepi.2009.04.001.

Hirth, G., and Kohlstedt, D.L., 2003, Rheology of the upper mantle and the mantle wedge: A view from the experimentalists, *in* Eiler, J., ed., Inside the Subduction Factory: American Geophysical Union Geophysical Monograph 138, p. 83–105, doi:10.1029/138GM06.

Humphreys, D.E., and Coblentz, D.D., 2007, North American dynamics and western U.S. tectonics: Reviews of Geophysics, v. 45, RG3001, doi:10.1029/2005RG000181.

Jové, C.F., and Coleman, R.G., 1998, Extension and mantle upwelling within the San Andreas fault zone, San Francisco Bay area, California: Tectonics, v. 17, p. 883–890, doi:10.1029/1998TC900012.

Karato, S.-I., Toriumi, M., and Fuji, T., 1980, Dynamic recrystallization of olivine single crystals during high-temperature creep: Geophysical Research Letters, v. 7, p. 649–652, doi:10.1029/GL007i009p00649.

Kohlstedt, D.L., Evans, B., and Mackwell, S.J., 1995, Strength of the lithosphere: Constraints imposed by laboratory experiments: Journal of Geophysical Research, v. 100, p. 587–617, doi:10.1029/95JB01460.

Lockner, D.A., Morrow, C., Moore, D., and Hickman, S., 2011, Low strength of deep San Andreas fault gouge from SAFOD core: Nature, v. 472, p. 82–85, doi:10.1038/nature09927.

Michibayashi, K., Ina, T., and Kanagawa, K., 2006, The effect of dynamic recrystallization on olivine fabric and seismic anisotropy: Insight from a ductile shear zone, Oman ophiolite: Earth and Planetary Science Letters, v. 244, p. 695–708, doi:10.1016/j.epsl.2006.02.019.

Molnar, P., 1992, Brace-Goetze strength profiles, the partitioning of strike-slip and thrust faulting at zones of oblique convergence, and the stress–heat flow paradox of the San Andreas fault, *in* Evans, B., and Wong, T.F., eds., Fault Mechanics and Transport Properties of Rocks: London, Academic Press, p. 435–459.

Nakata, J.K., et al., 1993, New radiometric ages and tephra correlations from the San Jose and the northeastern part of the Monterey 1:100,000 map quadrangles, California: Isochron/West, v. 60, p. 19–32.

Ozalaybey, S., and Savage, M.K., 1995, Shear wave splitting beneath the western United States in relation to plate tectonics: Journal of Geophysical Research, v. 100, p. 18,135–18,149, doi:10.1029/95JB00715.

Pollitz, F.F., Wicks, C., and Thatcher, W., 2001, Mantle flow beneath a continental strike-slip fault: Postseismic deformation after the 1999 Hector Mine earthquake: Science, v. 293, p. 1814–1818, doi:10.1126/science.1061361.

Prinzhofer, A., and Nicolas, A., 1980, The Bogota Peninsula, New Caledonia: A possible oceanic transform fault: The Journal of Geology, v. 88, p. 387–398, doi:10.1086/628523.

Regan, S.P., Williams, M.L., Leslie, S., Mahan, K.H., Jercinovic, M.J., and Holland, M.E., 2014, The Cora Lake shear zone, Athabasca granuilite terrane (Snowbird Tectonic Zone), an intraplate response to far-field orogenic processes during amalgamation of Laurentia: Canadian Journal of Earth Sciences, v. 51, p. 877–901, doi:10.1139/cjes-2014-0015.

Rybacki, E., and Dresen, G., 2004, Deformation mechanism maps for feldspar rocks: Tectonophysics, v. 382, p. 173–187, doi:10.1016/j.tecto.2004.01.006.

Scholz, C., 2000, Evidence for a strong San Andreas fault: Geology, v. 28, p. 163–166, doi:10.1130/0091-7613(2000)28<163:EFASSA>2.0.CO;2.

Shelly, R.D., 2015, Complexity of the deep San Andreas Fault zone defined by cascading tremor: Nature Geoscience, v. 8, p. 145–151, doi:10.1038/ngeo2335.

Teyssier, C., and Tikoff, B., 1998, Strike-slip partitioned transpression of the San Andreas fault system: A lithospheric-scale approach, *in* Holdsworth, R.E., et al., eds., Continental Transpressional and Transtensional Tectonics: Geological Society of London Special Publication 135, p. 143–158, doi:10.1144/GSL.SP.1998.135.01.10.

Titus, S.J., Medaris, G.L., Wang, H.F., and Tikoff, B., 2007, Continuation of the San Andreas fault system into the upper mantle: Evidence from spinel peridotite xenoliths in the Coyote Lake basalt, central California: Tectonophysics, v. 429, p. 1–20, doi:10.1016/j.tecto.2006.07.004.

Titus, S.J., Maes, S.M., Benford, B., Ferré, E.C., and Tikoff, B., 2011, Fabric development in the mantle section of a paleotransform fault and its effect on ophiolite obduction, New Caledonia: Lithosphere, v. 3, p. 221–244, doi:10.1130/L122.1.

Van der Wal, D., Chopra, P., Drury, M., and FitzGerald, J., 1993, Relationships between dynamically recrystallized grain size and deformation conditions in experimentally deformed olivine rocks: Geophysical Research Letters, v. 20, p. 1479–1482, doi:10.1029/93GL01382.

Vauchez, A., Tommasi, A., and Mainprice, D., 2012, Faults (shear zones) in the Earth's mantle: Tectonophysics, v. 558–559, p. 1–27, doi:10.1016/j.tecto.2012.06.006.

Warren, J.M., and Hauri, E.H., 2014, Pyroxenes as tracers of mantle water variations: Journal of Geophysical Research, v. 119, p. 1851–1881, doi:10.1002/2013JB010328.

Warren, J., and Hirth, G., 2006, Grain size sensitive deformation mechanisms in naturally deformed peridotites: Earth and Planetary Science Letters, v. 248, p. 438–450, doi:10.1016/j.epsl.2006.06.006.

Zoback, M.D., et al., 1987, New evidence on the state of stress of the San Andreas fault system: Science, v. 238, p. 1105–1111, doi:10.1126/science.238.4830.1105.

Manuscript received 5 March 2015
Revised manuscript received 22 June 2015
Manuscript accepted 28 July 2015

Printed in USA

Geology

Mantle strength of the San Andreas fault system and the role of mantle-crust feedbacks

Vasileios Chatzaras, Basil Tikoff, Julie Newman, Anthony C. Withers and Martyn R. Drury

Geology 2015;43;891-894
doi: 10.1130/G36752.1

Notes